DOI: 10.4408/IJEGE.2011-03.B-080

# DEVELOPMENT AND APPLICATION OF GUI EQUIPPED 1-D AND 2-D DEBRIS FLOW SIMULATOR, APPLIED TO MIXED-SIZE GRAINS

KANA NAKATANI(*), TAKASHI WADA(**), NAOKI MATSUMOTO(***), YOSHIFUMI SATOFUKA(****) & TAKAHISA MIZUYAMA(*****)

(*) JSPS Research Fellow, Graduate School of Agriculture, Kyoto University, Japan
(**) Affiliation River Engineering Group, Engineering Consultants NEWJEC Inc., Japan
(***) Himekawa Sabo Office, Nagano Prefecture, Japan
(****) Ritsumeikan University, Dept. of Civil Engineering, Japan
(*****) Graduate School of Agriculture, Kyoto University, Japan

## ABSTRACT

Debris flows often cause substantial losses to human life and the economy. The amount of damage can be effectively reduced using numerical simulation models, which can describe the debris-flow process and determine the possible effects of sabo dams or erosion and sediment control dams. Although various models have been developed, many existing debris-flow numerical simulations do not have efficient graphical user interfaces (GUIs). In addition, actual debris flows are composed of mixed grain-size sediment, which causes sediment sorting, while many simulation models have been developed only for uniform-sized gravel. Here, we report the development of a GUI-equipped oneand two-dimensional (1D and 2D, respectively) debris-flow simulation system for mixed-size gravel. The model uses two layers in 1D simulations to account for debris-flow sediment sorting, and can also examine the effect of closed, slit, and grid sabo dams. The model can incorporate multiple dams and combinations of different types of sabo dams. We simulated a debris-flow disaster that occurred on September 6, 2005, in Miyajima, Hiroshima Prefecture. Although two sabo dams were present along the torrent, a large amount of damage was caused in the nearby residential area. We considered these existing dams in our simulation. Our results demonstrated that applying the mixed grain-size sediment model provided a more realistic description of the debris-flow deposition than uniform-sized gravel models. Furthermore, our GUIequipped system enabled the user to input the data easily and to understand the results instinctively from the animated graphical results. Thus, the interface enables users to run high-quality debris-flow simulations easily and leads them to better solutions for sabo engineering.

***KEY WORDS**: debris flow, numerical simulation, mixed-size grains, sediment sorting, two-layer model, GUI, Miyajima area*

## INTRODUCTION

Debris flows often cause substantial losses to human life and the economy. The amount of damage can be effectively reduced using numerical simulation models, which can describe the debris-flow process (e.g., EGASHIRA *et alii*, 1997; TAKAHASHI, 2007) and determine the possible effects of sabo dams (e.g., SATOFUAKA & MIZUYAMA, 2005, 2006). Although various models have been developed, many existing debris-flow numerical simulations do not have efficient graphical user interfaces (GUIs). Therefore, we developed KANAKO and KANAKO 2D (NAKATANI *et alii*, 2007, 2008), general-purpose debris-flow simulation packages equipped with efficient GUIs, and applied them to real disasters and debris-flow torrents (NAKATANI *et alii*, 2009, 2010). However, actual debris flows are composed of mixed grain-size sediment, which causes sediment sorting (TAKAHASHI *et alii*, 2001). Some researchers have studied this phenomenon (e.g., DAVID, 1990; IVERSON, 2003), while many simulation models have been developed only for uniform-sized.

 

Here, we report the development of a GUI-equipped one- and two-dimensional (1D and 2D, respectively) debris-flow simulation system "KANAKO 2D Ver. 2.1" for mixed grain-size sediment. The model uses two layers in 1D simulations to account for debrisflow sediment sorting, and it can also examine the effect of sabo dams. We used the developed software package to simulate the debris-flow disaster that occurred on September 6, 2005, in Miyajima, Hiroshima Prefecture, and compared the results obtained using mixed and uniform grain-size sediment.

## METHODS

We developed our system using MS Visual Basic. NET (VB.NET). Our resulting software package contains two parts: a user interface that manages the data input and displays the output, and a simulation model. For the user interface, we applied and extended KANAKO 2D, which can simulate uniform-sized gravel. For the simulation model, we applied and modified an integrated model (WADA *et alii*, 2008) so that we could obtain more accurate results in the boundary area between 1D simulation areas, such as gullies, and 2D simulation areas, such as alluvial fans. We also modified a mixed grain-size gravel model (MATSUMOTO *et alii*, 2008).

By integrating and improving existing simulation models (SATOFUAKA & MIZUYAMA, 2005, 2006), users can easily simulate and examine the effect of closed, slit, and grid sabo dams.

## 1D AND 2D DEBRIS-FLOW SIMULATION MODEL APPLIED TO MIXED GRAIN-SIZE SEDIMENT

Our proposed model is based on an integration model for uniformsized gravel for 1D and 2D simulation areas. In 1D simulation areas, we applied a mixed grain-size gravel erosion/deposition process, and also considered sediment sorting and the concentration of coarse particles at the front of the debris flow (SATOFUAKA *et alii*, 2007). In 2D simulation areas, the vertical slope becomes gradual and the stress is distributed in the cross-flow direction. Therefore, since the exchange of particles in the vertical direction decreases, we excluded the process of sediment sorting and the concentration of coarse particles at the front of the debris flow.

The governing equations for the proposed model are given separately for 1D and 2D simulation areas in the following sections.

### *TWO-LAYER MODEL FOR 1D SIMULATION AREAS*

In 1D simulation areas, we applied a two-layer model as a simple means of representing the sorting phenomena. This model uses the basic equations for a one-layer debris-flow model with mixed materials, but the vertical change in the sediment concentration is also considered. The flow is divided into two vertical layers (see Fig. 1), and the proportion of each grain-size category of flowing sediment at each point is considered. Inverse gradient or sediment sorting is modeled by exchanging particles between layers. The process is calculated using parameters obtained from laboratory experiment results (see details from SATOFUAKA *et alii*, 2007).

We use the subscript $k$ to indicate the $k^{th}$ grain-size category. Therefore, $d_k$ and $C_k$ are the particle diameter and concentration, respectively, of the $k^{th}$ grain size. The average particle diameter $d_m$ in a debris flow that consists of mixed materials can be expressed as

$$d_m = \frac{C_1 d_1 + C_2 d_2 + \cdots + C_k d_k + \cdots + C_{ke} d_{ke}}{C_1 + C_2 + \cdots + C_k + \cdots C_{ke}} \quad (1)$$

where $ke$ is the largest grain-size category. Here, $C_k$, $d_k$, and $d_m$ represent the values of the total flow depth.

The vertical change in sediment concentration is considered using a new variable $p_k$, as shown in Fig. 2, that indicates the proportion of each grain-size category of flowing particles. Given the exchange of particles between the two layers, this proportion will

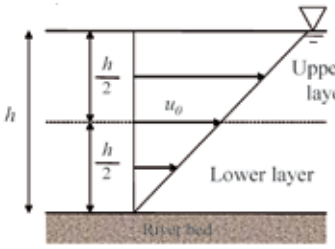


*Fig. 1 - Velocity distribution in the debris flow ($u_0$: average flow velocity for the total flow depth)*

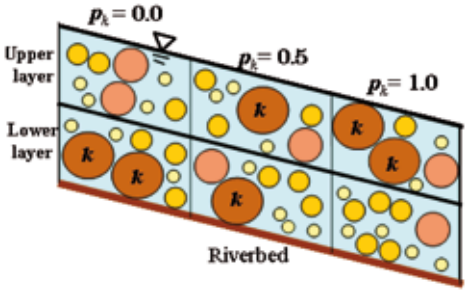


*Fig. 2 - Outline of particle proportion $p_k$ in the upper layer*

change with time, and is determined using

$$p_k = \frac{C_{U,k}}{C_{U,k} + C_{L,k}} \tag{2}$$

Here, the subscripts $U$ and $L$ indicate the upper and lower layers, respectively.

The total unit sediment discharge for the $k^{th}$ grain-size category in entire layer $q_{bk}$ is calculated as following;

$$q_{b,k} = u_0 h C_k \left( \frac{1}{2} + p_k \right) \tag{3}$$

Since the value of $p_k$ ranges between 0 and 1, $q_{bk}$ is affected by a change in concentration ranging from 0.5 to 1.5 times that of the uniform case. When we use Eq. (3) to solve the continuity equations for each grain-size category instead of the standard sediment flux formula, we can reproduce the concentration of larger particles at the front of the flow.

If a particle in the upper layer is sufficiently smaller than the average opening space in the lower layer $R_m$, it can move into the lower layer. However, a larger particle cannot enter the same opening, as shown in Fig. 3. MIDDLETON (1970) inferred that large particles are pushed upward when small particles fall into the openings between large particles (dynamic sieving). We considered that this is the main factor producing vertical sediment sorting. The average opening size of the lower layer can be expressed as follows using the average particle diameter in the lower layer:

$$R_m = k_1 d_{Lm} = k_1 \frac{\sum_{k=1}^{ke} d_k C_{L,k}}{\sum_{k=1}^{ke} C_{L,k}} \tag{4}$$

where $d_{Lm}$ is average particle diameter of the lower layer and $k_1$ is a coefficient.

The rate at which particles fall into openings in the lower layer is thought to increase when the proportion of small particles in the upper layer is large and the velocity is high. Therefore, the rate $r_k$ can be expressed as follows:

$$r_k = k_2 C_{U,k} |u_0| = 2 k_2 p_k C_k |u_0| \tag{5}$$

where $k_2$ is a coefficient. Equation (5) can be applied to smaller particle categories, $d_k < R_m$. Larger particle categories, $d_k \geq R_m$, must move upward to compensate for the downward movement of the smaller particles because of the assumption that the sediment is distributed homogeneously over the entire flow.

These movements cause the exchange of particles and vertical sorting in the debris flow. The rate $r'_k$ can be expressed as:

$$r'_k = k_3 C_{L,k} |u_0| = 2 k_3 (1 - p_k) C_k |u_0| \tag{6}$$

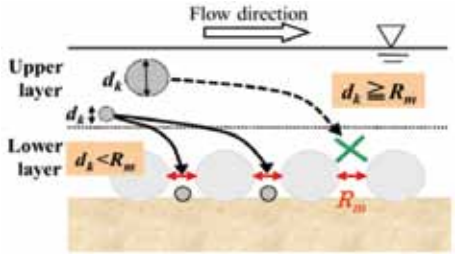


*Fig. 3 - Settling condition of small particles and large particles, depending on the opening space in the lower layer*

where $k_3$ is a coefficient.

From the results of laboratory experiments examining the size distribution of debris flow in the vertical direction, we set $k_1 = 0.75$ and $k_2 = 0.01$.

## *GOVERNING EQUATIONS FOR 1D SIMULATION AREAS*

The governing equations for 1D simulation areas are as follows. First, the continuity equation for the entire debris-flow volume is:

$$\frac{\partial h}{\partial t} + \frac{\partial uh}{\partial x} = \sum_{k=1}^{ke} i_k \tag{7}$$

The continuity equation for the $k^{th}$ grain-size category sediment volume for the entire flow is:

$$\frac{\partial C_k h}{\partial t} + \frac{\partial q_{bk}}{\partial x} = \frac{\partial C_k h}{\partial t} + \frac{\partial uh C_k \left( \frac{1}{2} + p_k \right)}{\partial x} = i_k C_* \tag{8a}$$

The continuity equation for the $k^{th}$ grain-size category sediment volume of the upper layer is:

$$\frac{\partial C_{U,k} \frac{h}{2}}{\partial t} + \frac{\partial q_{bU,k}}{\partial x} = \frac{1}{2} \frac{\partial C_{U,k} h}{\partial t} + \frac{3}{2} \frac{\partial uh p_k C_k}{\partial x} = \begin{cases} -r_k & (d_k < R_m) \\ r'_k & (d_k \geq R_m) \end{cases} \tag{8b}$$

The momentum equation for the debris flow in the flow direction (xaxis) can be expressed as:

$$\frac{\partial u}{\partial t} + u \frac{\partial u}{\partial x} = -g \frac{\partial H}{\partial x} - \frac{\tau}{\rho h} \tag{9}$$

Finally, the equation used to determine the change in the bed surface elevation is:

$$\frac{\partial z}{\partial t} + \sum_{k=1}^{ke} i_k = 0 \quad \left( \sum_{k=1}^{ke} i_k = i \right) \tag{10}$$

In Eqs (7)-(10), $i_k$ is the erosion/deposition velocity for the $k^{th}$ grainsize category, $u$ is the x-axis flow velocity, $z$ is the bed elevation, $t$ is time, $g$ is the acceleration due to gravity, $H$ is the flow surface elevation ($H = h + z$), $\rho$ is the interstitial fluid density, $C_*$ is the sediment concentration by volume in the movable bed layer, and $\tau_x$ is the riverbed shearing stresses in the $x$-axis direction.

 

When considering the continuity equation for the $k^{th}$ grain-size category sediment volume, we first calculate the continuity equation for the entire flow, and then we calculate the continuity equation for the upper layer. We determine the lower layer volume from the difference between the entire flow and the upper layer volumes. When sediment sorting does not occur, we set the falling rate and rising rate to 0; thus, we don't need to consider the continuity equation for the upper layer, and just model one layer of flow. Such a situation can occur when applying this model to uniform-sized grains or to bed load transport in mild-slope areas.

We apply the two-layer model to represent the sediment sorting phenomena. However, we do not calculate the flow motion of the upper and lower layers separately. Instead, we assume that the sediment concentration is distributed homogeneously in the flow depth direction, and we use the entire flow sediment concentration when calculating the momentum equation and the erosion/deposition process.

*EROSION / DEPOSITON VELOCITY*

The erosion and deposition process is related to the difference between the equilibrium sediment concentration $C_\infty$ and the actual sediment concentration C (Takahashi *et alii*, 1991a). If $C < C_\infty$, and $i < 0$, the deposition velocity is

$$i = \delta_d \frac{C_\infty - C}{C_*} \frac{q}{h} \tag{11}$$

where $q$ is a unit sediment discharge, $C_\infty$ is the equilibrium sediment concentration, $C$ is the sediment concentration of all the grain sizes in the flow, and $\delta_d$ is a deposition coefficient. The deposition velocity for the $k^{th}$ grain-size category $i_k$ is as follows:

$$i_k = i \frac{C_k}{C} \tag{12}$$

However, in Eq. (12), once erosion occurs and sediment is taken into the flow, the deposition due to particle settling is neglected, even in low gradient and velocity areas, such as the mouth of a river or upstream of a dam. Therefore, when the sediment diameter ($k^{th}$ grain-size number) is small and the flow reaches a low-velocity section so that the friction velocity $u_{*ck}$ is less than the settling velocity $w_{0k}$, we consider deposition due to the settling by adding the Rubey's settling velocity $w_{0k}$ as follows:

$$i_k = \begin{cases} -w_{0k} C_k + i \dfrac{C_k}{C} & (u_* < w_{ok}) \\ i \dfrac{C_k}{C} & (u_* \geq w_{ok}) \end{cases} \tag{13}$$

If $C > C_\infty$ and $i > 0$, the erosion velocity is:

$$i = \delta_e \frac{C_\infty - C}{C_* - C_\infty} \frac{q}{d_{mbed}} \tag{14}$$

where $\delta_e$ is the erosion coefficient and $d_{mbed}$ is the average particle diameter of the bed surface.

Whether particles of diameter $d_k$ are movable can be judged depending on the sediment transport movement. The deposition velocity for the $k^{th}$ grain-size category $i_k$ is as follows.

For debris flow and sediment sheet flow:

$$i_k = \begin{cases} if_{bk} & (d_k < h) \\ 0 & (d_k \geq h) \end{cases} \tag{15a}$$

For bed load transport, whether particles of diameter $d_k$ are movable can be judged by using a modified Egiazaroff's critical shear stress concept:

$$i_k = \begin{cases} if_{bk} & (u_* > u_{*ck}) \\ 0 & (u_* \leq u_{*ck}) \end{cases} \tag{15b}$$

where $f_{bk}$ is the volume ratio of the $k^{th}$ grain-size category particles to all the particles on the bed surface, $u_*$ is the shear stress $\sqrt{gh \tan \theta_w}$ (= , where $\theta_w$ is the slope of the water surface), and $u_{*ck}$ is the critical friction velocity of a $k^{th}$ grain-size category particle.

*EQUILIBRIUM SEDIMENT CONCENTRATION AND RIVERBED SHEARING STRESS*

The equations for equilibrium sediment concentration and riverbed shearing stress are based on previous research (Nakagawa & Takahashi, 1991a). The sediment transportation is classified as debris flow, sediment sheet flow, or bed load transport based on the slope gradient and sediment concentration of the flow.

*GRAIN SIZE DISTRIBUTION ON A RIVERBED SURFACE*

To calculate the erosion/deposition process for mixed grain-size sediment, we need to consider how the grain-size distribution of a riverbed surface varies with time. Therefore, we define a particleexchange layer $\delta_m$ above the riverbed surface, as shown in Fig. 4 (the layer thickness is constant), and consider that the grain-size distribution changes only in this layer. When erosion/deposition occurs and the riverbed surface changes, the particle-exchange layer will also change. On the upper surface of the particle-exchange layer, particle exchanges will occur through the fluid-phase erosion/deposition volume. On the lower surface of the particleexchange layer, particle exchange will occur through

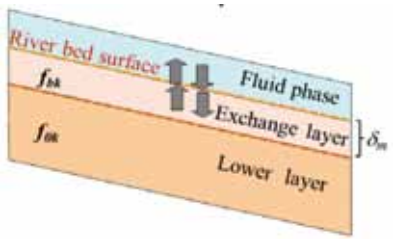


*Fig. 4 - Particle exchange layer for riverbed surfaces*

the lower layer, depending on how much the particle-exchange layer elevations have moved.

The time variation of the volume ratio of the $k^{th}$ grain-size category particles to all the particles on the bed surface, or the riverbed surface ratio $f_{bk}$, is as follows:

$$\frac{\partial f_{bk}}{\partial t} = \begin{cases} \dfrac{-i_k + if_{0k}}{\delta_m} & (i \geq 0) \\ \dfrac{-i_k + if_{bk}}{\delta_m} & (i < 0) \end{cases} \qquad (16)$$

where $f_{0k}$ is the volume ratio of the $k^{th}$ grain-size category particles to all the particles on the lower bed layer.

*EFFECT OF A SABO DAM*

As in the existing versions of KANAKO and KANAKO 2D, the user can prescribe three types of sabo dams for a 1D simulation area: closed, slit, or grid. For detail information of deposition process upstream to the sabo dam, see the following references (Satofuka & Mizuyama 2005, 2006; Nakatani *et alii*, 2008). For a grid sabo dam, the sediment material is composed of several grain-size classes, but we only consider the largest class of sediment, which blocks the grid dam opening and increases the dam height. In the future, we may divide the grain-size classes into two groups for grid sabo dams, and consider that the mean diameter of the larger group affects the dam blockage.

*2D SIMULATION AREAS*

In a 2D simulation area, the vertical slope is more gradual and the stress is distributed in the cross-flow direction. Therefore, since the exchange of particles in the vertical direction decreases, we excluded the process of sediment sorting and the concentration of coarse particles at the front of the debris flow. We apply the particle-number conservation law (Takahashi *et alii*, 1991b) to calculate the change in time and space of the mean particle size $d_m$ in the flow, and then calculate the other variables assuming a uniform grain size and making use of the calculated $d_m$:

$$\frac{\partial}{\partial t}\left(\frac{Ch}{d_m^3}\right) + \frac{\partial}{\partial x}\left(\frac{Cuh}{d_m^3}\right) + \frac{\partial}{\partial y}\left(\frac{Cvh}{d_m^3}\right) = \frac{iC_*}{d_m^3} \qquad (17)$$

The governing equations for 2D simulation areas are same as those for 1D simulation areas, but they consider the cross ($y$-axis) direction as well as the flow ($x$-axis) direction. We only modeled uniform grain-size and one layer flow in 2D simulation areas, calculated using Eq. (17).

## KANAKO 2D VER. 2.10: A GUI-EQUIPPED 1D AND 2D DEBRIS-FLOW SIMULATOR APPLIED TO MIXED GRAIN-SIZE SEDIMENT

As in the existing version of KANAKO 2D for uniform grain-size sediment simulations, a longitudinal figure representing the 1D riverbed profile, and a plane figure displaying the 1D river width and 2D landform plane appears. The debris flow first passes through the 1D simulation area, and then through the 2D simulations area. The KANAKO 2D GUI system is also easy to use for beginners because the required simulation data sets can be input using a mouse and viewed on a monitor. A new function for mixed grain-size sediment is the grain-size detail-setting screen, which is used to set the grain-size classifications, grain diameter, and concentration of particles in the supplied hydrograph. A data file is used to set the volume ratio of riverbed particles.

During simulations, users can view real-time images of the simulation results on the main screen and the 2D landform screen. On the main screen, the user can see real-time images of the flow depth and riverbed variation in the longitudinal and plane plots. Users can also visualize the flow and sediment discharge at each calculation point. The new mixed grain-size sediment function allows the user to visualize the discharge of each grain-size classification of sediment along with the entire sediment discharge. Users can also view real-time images of the average particle diameter on the 2D landform screen during the simulations, as it is shown in Figs. 8. Other functions are the same as those in the existing KANAKO 2D interface (see Nakatani *et alii*, 2010).

## SYSTEM APPLICATION TO A REAL DEBRIS-FLOW DISASTER

On September 6, 2005, a debris flow occurred on Miyajima, a small island in Hiroshima Prefecture, Japan (Kaibori *et alii*, 2006). Landslides followed heavy typhoon rains, and the accumulated debris and rocks gathered and flowed down about 2.6 km, destroying

 

two existing closed sabo dams and causing sediment to overflow downstream. We simulated this event using the developed KANAKO 2D Ver. 2.10 package by modeling the mixed grain-size sediment debris flow.

*SIMULATION CONDITIONS*

The total volume of sediment resulting from the failure was an estimated 18,000 m³. Therefore, we supplied this sediment amount as the initial debris flow volume from the upstream end of the simulation. We then calculated the sediment concentration of the slope after applying the Takahashi equation (TAKAHASHI *et alii*, 2001) for the equilibrium concentration of debris flow:

$$Cd = \frac{\rho \tan\theta}{(\sigma - \rho)(\tan\phi - \tan\theta)} \quad (16)$$

where $\sigma$ is the mass density of the bed material (= 2550 kg/m³); $\rho$ is the mass density of the fluid phase including water, mud, and silt (= 1180 kg/m³); $\phi$ is the internal friction angle (= 35°); $\theta$ is the angle of the 100-m slope area (= 4.93°); $Cd$ is the concentration of the debris flow ($0.3 \le Cd \le 0.9C_*$); and $C_*$ is the concentration of the movable bed (= 0.6).

We obtained a debris-flow concentration of 30% from Eq. (18). Then, we calculated the peak debris-flow discharge using the following equations from the Sabo Master Plan for Debris Flow (NILIM Japan, 2007):

$$Q_{sp} = 0.01\sum Q \quad (19)$$

$$\sum Q = \frac{Vdqp \cdot C_*}{Cd} \quad (20)$$

where $Q_{sp}$ is the peak debris-flow discharge (m³/s), $\Sigma Q$ is the entire debris-flow volume including water and sediment (m³), and $Vdqp$ is the sediment volume (m³).

The total calculated debris-flow volume was 36,000 m³, and the peak debris-flow discharge was 360 m³/s. The supplied debris-flow conditions are illustrated in Fig. 5. Reportedly, 13,000 m³ of sediment was moved from the riverbed during the erosion process and transported downstream. Therefore, we placed 13,000 m³ (including void) of sediment evenly distributed along the riverbed. Using the landform data, the calculated thickness was 0.7 m. The landform conditions were obtained from topographic maps and reports, and were prescribed in KANAKO 2D as shown in Fig. 6. We set the river width for the 1D landform area at a constant 15 m. Other parameters were set as listed in Table 1.

We considered two grain-size conditions in the supplied hydrograph and initial riverbed ratio (see Table 2). In Case 1, we used ten grain-size classifications with equal proportions. In Case 2, we set a uniform grain size of 0.55 m, which was the average diameter for

| Parameters/Variables | Value | Unit |
|---|---|---|
| Simulation time | 1800 | s |
| Time step | 0.01 | s |
| Mass density of bed material $\sigma$ | 2550 | kg/m³ |
| Mass density of fluid (water and mud, silt) phase $\rho$ | 1180 | kg/m³ |
| Concentration of movable bed $C_*$ | 0.6 | |
| Internal friction angle $\tan\phi$ | 0.7 | |
| Acceleration of gravity | 9.8 | m/s² |
| Coefficient of erosion rate | 0.0007 | |
| Coefficient of accumulation rate | 0.05 | |
| Manning's roughness coefficient | 0.03 | s/m$^{1/3}$ |
| Number of 1-D calculation points | 61 | |
| Interval of 1-D calculation points | 20 | m |
| Number of 2-D calculation points | 60 x 60 | |
| Interval of 2-D calculation points | 8.47 x 8.47 | m |

*Tab. 1 - Simulation parameters*

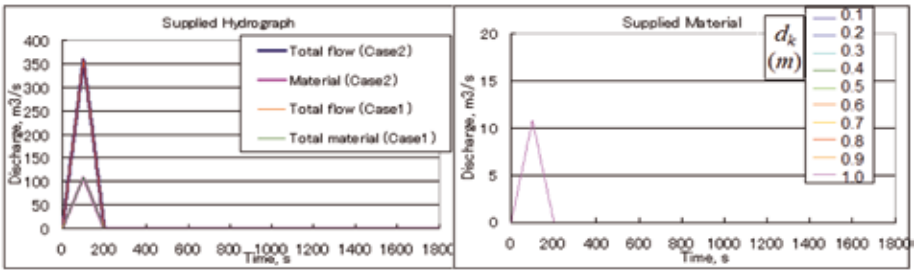


*Fig. 5 - Supplied hydrograph for Cases 1 and 2 (left figure) and supplied material conditions for Case 1 (right figure)*

| | Case 1 | | | | | | | | | | Case 2 |
|---|---|---|---|---|---|---|---|---|---|---|---|
| Grain diameter (m) | 0.1 | 0.2 | 0.3 | 0.4 | 0.5 | 0.6 | 0.7 | 0.8 | 0.9 | 1.0 | 0.55 |
| Supplied sediment concentration | 0.03 | 0.03 | 0.03 | 0.03 | 0.03 | 0.03 | 0.03 | 0.03 | 0.03 | 0.03 | 0.3 |
| Ratio in initial riverbed | 0.1 | 0.1 | 0.1 | 0.1 | 0.1 | 0.1 | 0.1 | 0.1 | 0.1 | 0.1 | 1.0 |

*Tab. 2 - Simulation cases*

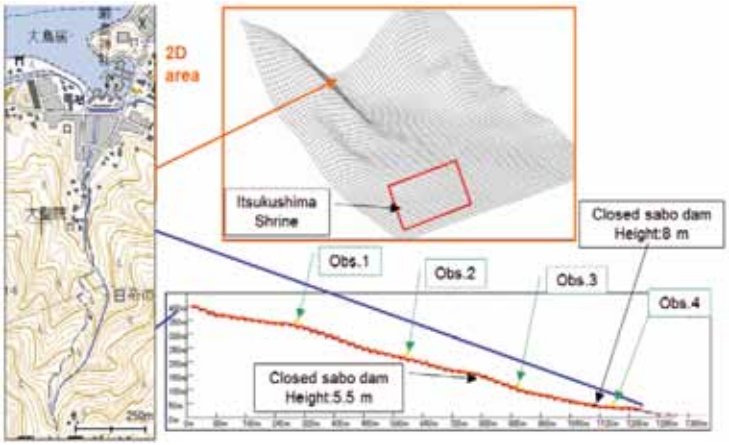


*Fig. 6 - Miyajima simulation area shown on KANAKO 2D (1D area in the lower right, 2D area in the upper right) and corresponding topography map (left)*

Case 1. We included the two existing sabo dams in the simulations, and assumed that both dams were empty.

*SIMULATION RESULTS FOR 1D AREA*

We compared the total flow and sediment discharge for both cases at the four observation points labeled in Fig. 8 as Obs. 1-4. We also examined each grain size sediment discharge for Case 1 (see Fig.6). At Obs. 1, the difference between the total flow and total sediment discharge for the two cases was small. The grain size distribution for Case 1 indicated that the discharge of smaller sediments that were 0.1 and 0.2 m in diameter was higher than that of larger diameter sediments due to the selective transport caused by the flow velocity and flow depth.

At Obs. 1, the distance from the upstream end of the simulated flow was about 300 m and the gradient was not large, so the amount of flow was small and the flow depth was low, therefore sediment sorting did not occur.

At Obs. 2, the distance from the upstream end of the simulated flow was 600 m and the gradient was large, so the type of sediment transport was debris flow. Due to erosion of the initial riverbed, the sediment discharge in both Cases 1 and 2 increased compared to Obs. 1, and the amount of flow increased. Case 1 showed slightly more total sediment discharge and total flow, and the peak arrival time was slightly earlier than in Case 2. For Case 1, for larger sediments 0.5-1.0 m in diameter, the amount of discharge of each grain size was initially large over short periods of time. For smaller sediments 0.1-0.4 m in diameter, the amount of discharge was initially small, but this increased after the discharge of larger sediments decreased, and the duration of the discharge was longer than what was observed for the larger sediments. Therefore, sediment sorting occurred at Obs. 2.

The same tendency was observed at Obs. 3 and 4. A 5.5-m-high closed sabo dam was located between Obs. 2 and 3. This dam was not large enough for the amount of sediment and was located on a steep gradient, so it was not very effective. Due to erosion of the initial riverbed and the sediments flowing over the sabo dam, both Cases 1 and 2 predicted more sediment discharge and total flow at Obs. 3 than at Obs. 2. The trends for total sediment discharge, amount of flow, and sediment sorting were the same as seen at Obs. 2. A 8-m-high closed sabo dam was located between Obs. 3 and 4. This dam was also not large enough to catch all the sediment. However, the dam was located on a small gradient and its capacity was larger than the upper sabo dam, so it did trap some sediment. The slope gradient at this point was decreasing; thus, the sediment discharge and total flow were less at Obs. 4 compared to Obs. 3. As before, Case 1 predicted more total sediment discharge and total flow than Case 2, and the peak arrival time was slightly earlier.

The discharge peak of larger sediments 0.6-1.0 m in diameter was initially larger over short periods of time, as observed at Obs. 2 and 3. However, medium-sized sediments 0.3-0.5 m in diameter had a higher discharge peak than larger sediments over a short period of time. For smaller sediments 0.1-0.2 m in diameter, the amount of discharge was initially small, but this increased after the discharge of the larger and medium-sized sediments decreased and the duration of the discharge was longer. These phenomena occurred due to sediment sorting as the debris flow traveled down the slope, and due to deposition caused by the sabo dam and the decreasing slope gradient.

 

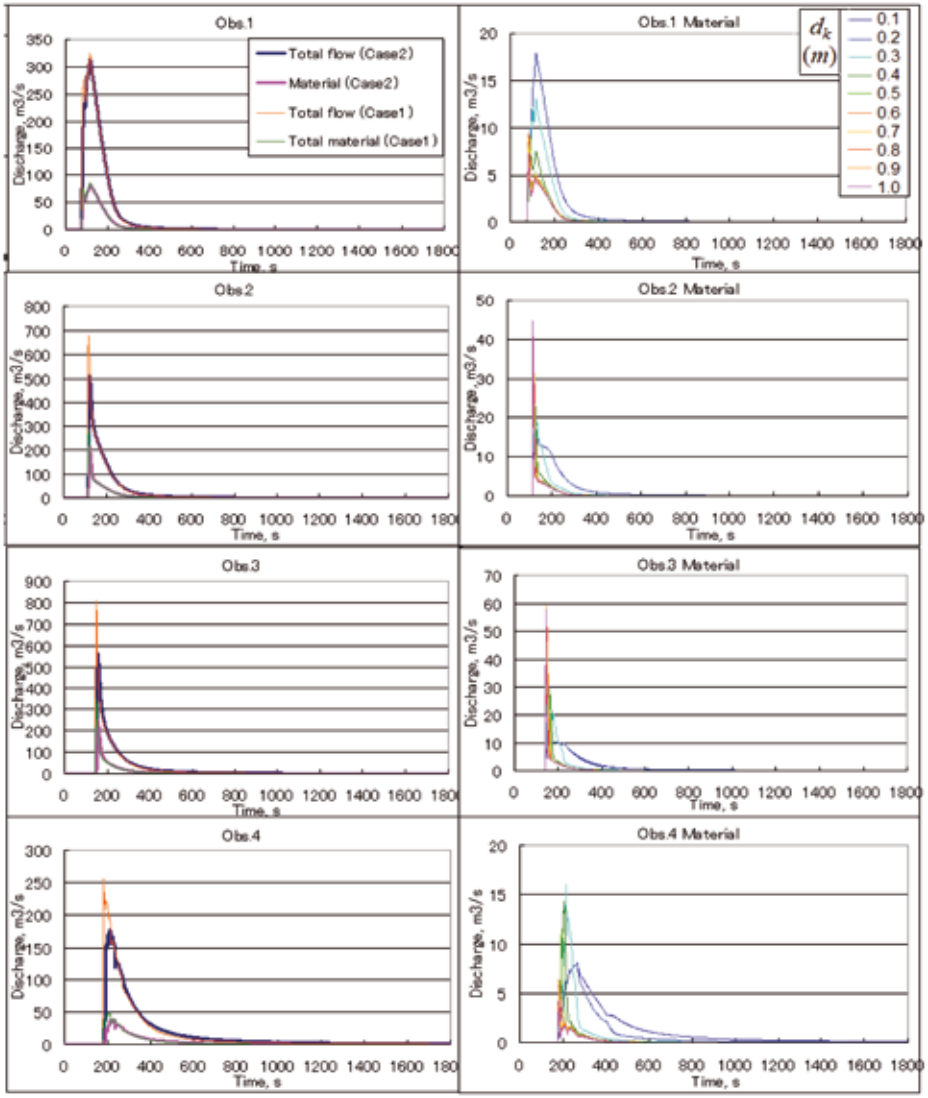


*Fig. 7 - Total flow and total sediment discharge for Cases 1 and 2 (left) and grain size sediment discharge for Case 1 (right)*

*SIMULATION RESULTS FOR 2D AREA*

We compared the riverbed variation over the 2D landform area for Cases 1 and 2 (shown in Fig. 8 center and right), at 301 s, 426 s, 645 s, and 1799 s. Case 1 with mixed grain-size sediment covered a wider area and the sediment deposition was thicker. This tendency was seen all through the simulation period 1800 s.

The transitional change of the average grain-size diameter is shown for Case 1, at 301 s, 426 s, 645 s, and 1799 s (shown in Fig. 8 left). The average grain-size diameter decreased with time due to sediment sorting. Also, the coarse particles were concentrated at the front of the debris flow in the 1D landform area, which affected the discharge flowing to the 2D area.

## CONCLUSION

By applying a mixed grain-size sediment model to debris-flow simulation, now we can describe the flow and erosion/deposition process of debris flows considering granularity characteristics. By equipping the mixed grain-size sediment simulation model with an efficient GUI, users can run more reasonable debris-flow simulations without difficulty, and are able to plan better sabo engineering solutions. We applied our

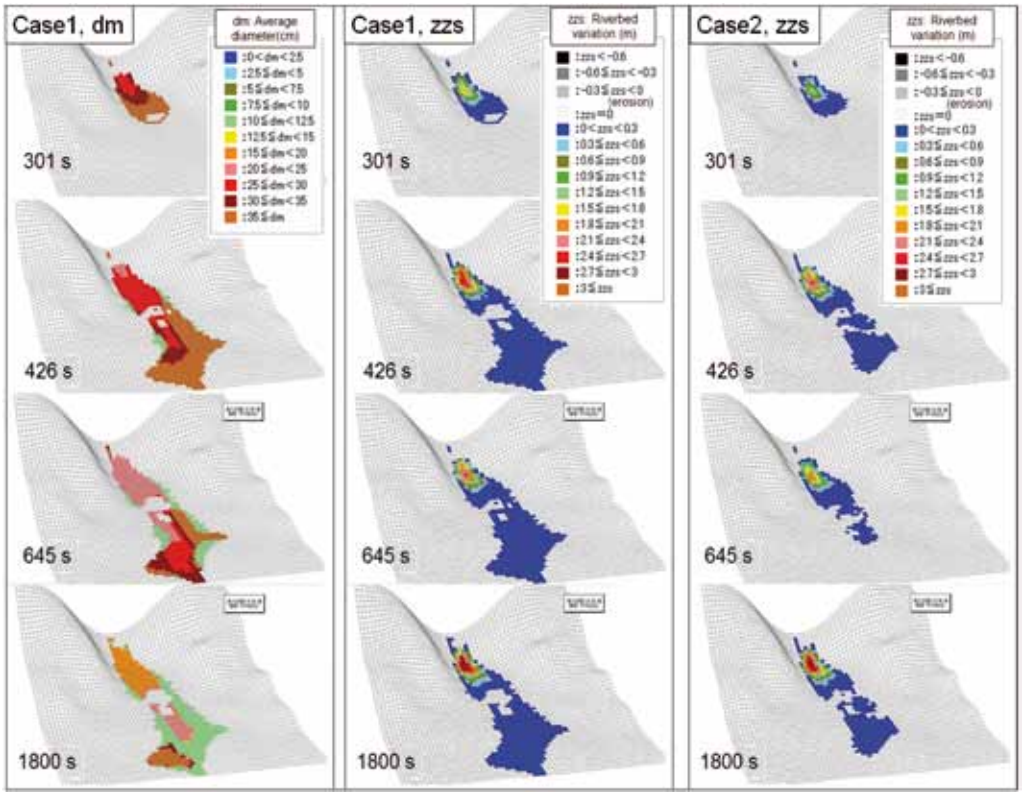


*Fig. 8 - Transitional change of average grain-size diameter in the 2D landform area for Case 1(left), riverbed variation in the 2D landform area for Case 1 (center) and Case 2 (right)*

system to a real debris-flow disaster that occurred in Japan and compared the results obtained using mixed and uniform grain-size sediment.

The results showed that the mixed grain-size sediment debris-flow predictions had higher discharges and earlier peak arrival times.

The results also showed differences in the deposition process in 2D areas, which correspond to residential areas. However, our proposed mixed grain-size sediment model is limited by the conditions of laboratory experiments; further studies are required to improve the parameters we used and check our assumptions. The proposed model should also be applied to other real disasters to ensure its accuracy. Furthermore, we must consider more userfriendly GUIs for the simulations.

## REFERENCES

Davies T. (1990) - *Debris-Flow Surges - Experimental Simulation.* Journal of Hydrology (NZ), **29**(1): 18-46.

Egashira S., Miyamoto K. & Itoh T. (1997) - *Constitutive equations of debris flow and their applicability*. Proc. 1st International Conference on Debris Flow Hazards Mitigation, ASCE: 340-349.

Iverson R.M. (2003) - *The debris-flow rheology myth*. Proceedings of the 3rd International Conference on Debris-Flow Hazard Mitigation: Prediction and Assessment, Millpress: 303-314.

Kaibori M., Ura M., Yoshimura M. & Fujimoto E. (2006) -*Debris flow disaster on September 6, 2005 in Miyajima, Hiroshima Prefecture*. Journal of the JSECE, Japan Society of Erosion Control Engineering , **58**(5): 18-21.

Matsumoto N., Wada T., Satofuka & Y. & Mizuyama, T. (2008) -*Prediction of debris flow deposition by a numerical model considering the change of grain size distribution*, Proc. 2008 Annual Conference of the JSECE, Japan, JSECE Publication No. **50**: 378-379.

Middleton G.V. (1970): *Experimental studies related to problems of flysch sedimentation. Flysch Sedimentology in North America.* Geol. Assoc. Can. Spec. Pap. **7**: 253-272.

 

Nakatani K., Satofuka Y. & Mizuyama T. (2007) - *Development of 'KANAKO', a wide use debris flow simulator equipped with GUI*, Proc. of 32nd Congress of IAHR, Venice, Italy: **10** p, A2.c-182.

Nakatani K, Wada T., Satofuka Y. & Mizuyama T.(2008) - *Development of "Kanako", a wide use 1-D and 2-D debris flow simulator equipped with GUI, Monitoring, Simulation, Prevention, and Remediation of Dense and Debris Flow II*, wit press: 49-60.

Nakatani K., Wada T., Satofuka Y. & Mizuyama T. (2010) - *Studies on development and application of general-purpose debris flow simulation system equipped with GUI*. Proc. of International Workshop on Multimodal Sediment Disasters Triggered by Heavy Rainfall and Earthquake and the Countermeasures, Yogyakarta, Indonesia: 197-206.

National Institute for Land and Infrastructure Management, Ministry of Land, Infrastructure and Transport, Japan (2007) -*Manual of Technical Standard for establishing Sabo master plan for debris flow and driftwood*. Technical Note of National Institute for Land and Infrastructure Management, Report.**364.**

Satofuka, Y. & Mizuyama T. (2005) - *Numerical simulation of a debris flow in a mountainous river with a sabo dam*. JSECE, **58** (1): 14-19.

Satofuka Y. & Mizuyama T. (2006) - *Numerical simulation of debris flow control by a grid dam*. Proc. of the 6th Japan-Taiwan Joint Seminar on Natural Hazard Mitigation

Satofuka Y., Iio T. & Mizuyama T. (2007) - *Sediment sorting in stony debris flow*. Proceedings of the 4th International Conference on Debris- Flow Hazards Mitigation: Mechanics, Prediction, and Assessment.

Sumaryono, Nakatani K, Satofuka Y. & Mizuyama T. (2009) - *One-dimensional numerical simulation for sabo dam planning using Kanako (Ver. 1.40): A case study at Cipanas, Guntur Volcanoes, West Java, Indonesia*, International JSECE, **2**(1): 22-32.

Takahashi T. & Nakagawa H. (1991a) - *Prediction of stony debris flow induced by severe rainfall*. Journal of the JSECE, **44** (3): 12-19.

Takahashi T., Nakagawa H. & Yamashiki Y. (1991b) - *Formation and erosion of debris fan that is composed of sediment mixture.* Annuals, DPRI, 34, B-2: 355-372.

Takahashi,T., Nakagawa H., Satofuka Y. & Kawaike K. (2001) - *Flood and sediment disasters triggered by 1999 rainfall in Venezuela: A river restoration plan for an alluvial fan.* Journal of Natural Disaster Science, **23**: 65-82.

Takahashi T. (2007): *Debris flow: Mechanics, Prediction and Countermeasures*. Taylor & Francis, Leiden